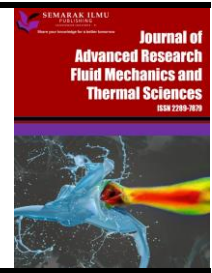




Journal of Advanced Research in Fluid Mechanics and Thermal Sciences

Journal homepage:
https://semarakilmu.com.my/journals/index.php/fluid_mechanics_thermal_sciences/index
ISSN: 2289-7879



Mixed Convection Nanofluid Flow using Lie Group Scaling with the Impact of MHD, Radiation, Thermophoresis and Brownian Motion over a Vertical Wedge

Pranitha Janapatla^{1,*}, Anomitra Chakraborty¹

¹ Department of Mathematics, National Institute of Technology Warangal-506004 Telangana, India

ARTICLE INFO

Article history:

Received 7 June 2022

Received in revised form 8 November 2022

Accepted 21 November 2022

Available online 11 December 2022

Keywords:

Mixed convection; radiation parameter;
Lie group scaling; vertical wedge;
nanofluid; MHD

ABSTRACT

The present study concerns with the mixed convection nanofluid flow across a vertical wedge with Radiation, MHD, Brownian motion, thermophoresis effects using Lie Group scaling analysis. The governing set of highly nonlinear partial differential equations are non-dimensionalized through appropriate transformations and transformed into ordinary differential equations using Lie Group Scaling, which is solved numerically using Shooting method along with *bvp4c* scheme. The radiation heat flux approximated with the Rosseland approximation has been implemented in the flow equations. The influence of mixed convection, magnetic, Brownian motion, radiation, Lewis number and thermophoresis parameter on the flow profiles are examined. For establishing the efficiency of our adopted numerical technique, we made comparisons with the earlier published works and we found them to be in very good agreement.

1. Introduction

One of the most important concepts in fluid dynamics, which is attracting researchers in recent decades is mixed convection flow and few of them has analyzed it on various flow models. Gorla *et al.*, [1] conducted studies for vertical surfaces in porous mediums with non-Newtonian fluid. The term "Nanotechnology", shorted to "Nanotech" was introduced in 1974 which later became much interesting for its varying uses. Dealing with nano-meter size objects varying between 1 to 100 nm is dealt in the field of Nanotech. The nano particles, which utilized in nanofluids are regularly used to make metals. It is also used in the field of electronics and energy along with fields of medical sciences for making health products. The study of nanofluids with various geometries and effects has been studied by various researchers such as Reddy and Chamkha [2], Selimefendigil and Öztöp [3], Khan and Pop [4], Turkyilmazoglu [5]. Khan *et al.*, [6], Nield and Bejan [7], and Khan *et al.*, [12] carried out their studies for different geometries. Murthy and Singh [8] is one of many authors who studied

* Corresponding author.

E-mail address: pranitha@nitw.ac.in

<https://doi.org/10.37934/arfmts.101.2.8598>

about thermal dispersion and Yen *et al.*, [23] is one of the few researchers to discuss about the governing equations in CFD. Study of MHD flows has gained a lot of popularity in the research world and it has been studied by various researchers such as Khan *et al.*, [24], Asghar and Teh [25], Bakar and Soid [26], Thirupathi *et al.*, [27] and Akaje and Olajuwon [28]. The radiation effect is also an essential key in heat and mass transfer due to its uncountable core applications in physics, engineering, industrial processes like nuclear power plants, gas turbines, thermal energy storage, glass production, furnace design, polymer processing, gas-cooled nuclear reactor and various branches of science and technology. Mixed convection flow under the magnetic field impact also earned attention in engineering and industrial applications such as magnetohydrodynamic power generators, magnetic drug targeting, petroleum industry. The study of mixed convection with variable properties heated with Lie Group method was considered by Pranitha *et al.*, [9]. Similar studies have been conducted by Meena and Pranitha [10] considering non-Darcy media for a power law nanofluid. Further analysis on MHD flows and heat transfer has been studied by authors like Cavallini *et al.*, [18], Divya *et al.*, [19], Prasad *et al.*, [20], and Vaidya *et al.*, [21,22].

The effects of radiation, magnetic effect, Brownian motion and thermal dispersion on the mixed convection nanofluid flow over a vertical wedge has not been studied earlier by any researcher. This is significant because the concepts of mixed convection on nanofluids find its wide range of applications in thermal engineering equipment, in the structure of cooling devices for electronics and microelectronic equipment, solar energy collection and thus the effects like radiation, thermophoresis is directly affecting the viscosity, velocity profiles, and also volume fraction in the above-mentioned field of applications. In this paper we aim to obtain the non-dimensional forms of the partial differential equations and later using similarity transformations and Lie group analysis we are obtaining the final set of equations [14]. These are numerically solved using the shooting method with *bvp4c* function. All the parameters have been reviewed closely and its effects on the heat and mass transfer coefficients were studied in this article. Such problems can be realized in the field of engineering developments and industrial uses.

2. Mathematical Formulation

The model on convective transport in nanofluids, incorporating different effects was introduced by Buongiorno [11]. Effects studied were Brownian diffusion and Thermophoresis. Collisions among particles of a fluid is caused due to their zig zag motion and is termed as Brownian motion. The difference in temperatures causes dispersal of particles of the fluid which is known as thermophoresis. Base equations for the nanofluid model are presented by Buongiorno model has been used in various flow models including this study.

$$\nabla \cdot \vec{q} = 0 \tag{1}$$

$$\frac{\partial \vec{q}}{\partial \bar{t}} + \vec{q} \cdot \nabla \vec{q} = -\frac{1}{\rho_f} \nabla p + \nu \nabla^2 \vec{q} + g(1 - \bar{\phi}_\infty) \beta_{\bar{T}} (\bar{T} - \bar{T}_\infty) - (\rho_p - \rho_f) g (\bar{\phi} - \bar{\phi}_\infty) \tag{2}$$

$$\frac{\partial \bar{T}}{\partial \bar{t}} + \vec{q} \cdot \nabla \bar{T} = \alpha \nabla^2 \bar{T} + \frac{(\rho c)_p}{(\rho c)_f} \left[D_B \nabla \bar{\phi} \cdot \nabla \bar{T} + \frac{D_T}{\bar{T}_\infty} \nabla \bar{T} \cdot \nabla \bar{T} \right] \tag{3}$$

$$\frac{\partial \bar{\phi}}{\partial \bar{t}} + \vec{q} \cdot \nabla \bar{\phi} = D_B \nabla^2 \bar{\phi} + \frac{D_T}{\bar{T}_\infty} \nabla^2 \bar{T} \tag{4}$$

Considering this model in Figure 1 where we have ε as the porosity and K being permeability of the medium. $\bar{T}_w, \bar{T}_\infty$ being the temperature at the wedge surface and away from wedge at long distances respectively. $\bar{\phi}_w, \bar{\phi}_\infty$ are the nanoparticle volume fraction at the surface of the wedge and at long distances from the wedge respectively.

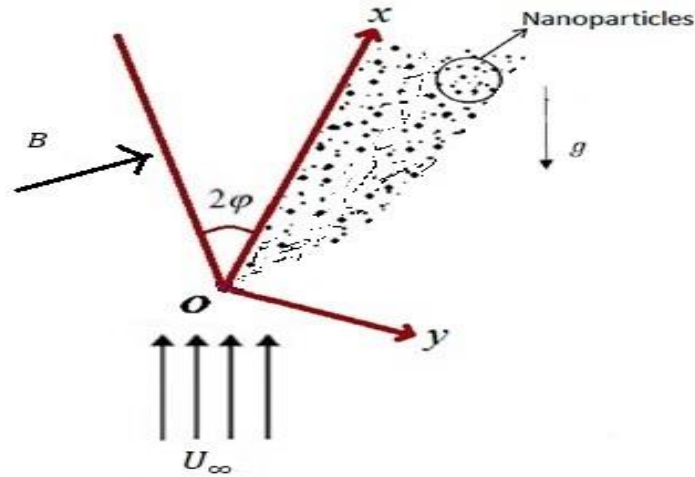


Fig. 1. Modelling of the present problem

On applying the linear Boussinesq approximations with other presumptions, the present model governing equations have been modified from the studies conducted by Chamkha *et al.*, [15] and Ganga *et al.*, [17] and is written as

$$\frac{\partial \bar{u}'}{\partial \bar{x}'} + \frac{\partial \bar{v}'}{\partial \bar{y}'} = 0 \quad (5)$$

$$\left[1 + \frac{\sigma \mu_e B^2 K}{\rho \nu} \right] \frac{\partial \bar{u}'}{\partial \bar{y}'} = \frac{(1 - \bar{\phi}_\infty) \rho_{f\infty} g_x K \beta}{\mu} \frac{\partial \bar{T}}{\partial \bar{y}'} - \frac{(\rho_p - \rho_{f\infty}) g_x K}{\mu} \frac{\partial \bar{\phi}}{\partial \bar{y}'} \quad (6)$$

$$\bar{u}' \frac{\partial \bar{T}}{\partial \bar{x}'} + \bar{v}' \frac{\partial \bar{T}}{\partial \bar{y}'} = \frac{\partial}{\partial \bar{y}'} \left[\alpha \frac{\partial \bar{T}}{\partial \bar{y}'} - \frac{1}{\rho c_p} q_y^r \right] + \tau \left[D_B \frac{\partial \bar{T}}{\partial \bar{y}'} \frac{\partial \bar{\phi}}{\partial \bar{y}'} + \frac{D_T}{\bar{T}_\infty} \left(\frac{\partial \bar{T}}{\partial \bar{y}'} \right)^2 \right] \quad (7)$$

$$\bar{u}' \frac{\partial \bar{\phi}}{\partial \bar{x}'} + \bar{v}' \frac{\partial \bar{\phi}}{\partial \bar{y}'} = \varepsilon \left[D_B \frac{\partial^2 \bar{\phi}}{\partial \bar{y}'^2} + \frac{D_T}{\bar{T}_\infty} \left(\frac{\partial^2 \bar{T}}{\partial \bar{y}'^2} \right) \right] \quad (8)$$

Along with B.C.'s as

$$\bar{v}' = 0; \quad \bar{T} = \bar{T}_w; \quad \bar{\phi} = \bar{\phi}_w \quad \text{at } \bar{y}' = 0 \quad (9)$$

$$\bar{u}' = U_\infty; \quad \bar{T} = \bar{T}_\infty; \quad \bar{\phi} = \bar{\phi}_\infty \quad \text{for } \bar{y}' \rightarrow \infty \quad (10)$$

Here $\tau = \frac{\varepsilon(\rho c)_p}{(\rho c)_f}$, $\alpha = \alpha_m + \gamma d \bar{u}'$, where α_m is the molecular thermal diffusivity and $\gamma d \bar{u}'$ is the thermal dispersion.

The radiative heat flux term applying Rosseland approximation [13] is written as

$$q_y^r = - \frac{4\sigma_0}{3k^*} \frac{\partial \bar{T}^4}{\partial \bar{y}'} \quad (11)$$

where σ_0 is Stefan - Boltzman constant while k^* being average absorption coefficient. Introducing the process of non-dimensionalization via the following variables

$$\begin{aligned} x &= \frac{\bar{x}'}{L}; & y &= \frac{Pe^{1/2}\bar{y}'}{L}; & u &= \frac{L\bar{u}'}{\alpha_m Pe}; & v &= \frac{L\bar{v}'}{\alpha_m Pe^{1/2}} \\ \theta &= \frac{\bar{T} - \bar{T}_\infty}{\bar{T}_w - \bar{T}_\infty}; & f &= \frac{\bar{\phi} - \bar{\phi}_\infty}{\bar{\phi}_w - \bar{\phi}_\infty} \end{aligned} \quad (12)$$

Introducing the stream function ψ and using its definition we have

$$u = \frac{\partial \psi}{\partial y}; \quad v = -\frac{\partial \psi}{\partial x} \quad (13)$$

Enforcing the Eq. (10) to Eq. (12) into the Eq. (6) to Eq. (8) and getting the residuals as

$$\varphi_1 = (1 + M^2) \frac{\partial^2 \psi}{\partial y^2} - \lambda \frac{\partial \theta}{\partial y} + Nr \lambda \frac{\partial f}{\partial y} \quad (14)$$

$$\varphi_2 = \frac{\partial \psi}{\partial y} \frac{\partial \theta}{\partial x} - \frac{\partial \psi}{\partial x} \frac{\partial \theta}{\partial y} - \frac{\partial^2 \theta}{\partial y^2} - Pe_\gamma \left(\frac{\partial^2 \psi}{\partial y^2} \frac{\partial \theta}{\partial y} + \frac{\partial^2 \theta}{\partial y^2} \frac{\partial \psi}{\partial y} \right) - Nb \frac{\partial f}{\partial y} \frac{\partial \theta}{\partial y} - Nt \left(\frac{\partial \theta}{\partial y} \right)^2 - \frac{4}{3} R \frac{\partial}{\partial y} \left((C_T + \theta)^3 \frac{\partial \theta}{\partial y} \right) \quad (15)$$

$$\varphi_3 = \frac{\partial \psi}{\partial y} \frac{\partial f}{\partial x} - \frac{\partial \psi}{\partial x} \frac{\partial f}{\partial y} - \frac{1}{Le} \frac{\partial^2 f}{\partial y^2} - A \frac{\partial^2 \theta}{\partial y^2} \quad (16)$$

Eq. (9) and Eq. (10) is transformed as

$$\psi = 0; \quad \theta = 1; \quad f = 1 \quad \text{at } y = 0 \quad (17)$$

$$\frac{\partial \psi}{\partial y} = 1; \quad \theta = 0; \quad f = 0 \quad \text{as } y \rightarrow \infty \quad (18)$$

2.1 Implementation of Lie Group of Transformations

Introducing the following change of coordinates

$$\begin{aligned} \Gamma: x^* &= x e^{\epsilon \zeta_1}, & y^* &= y e^{\epsilon \zeta_2} \\ \psi^* &= \psi e^{\epsilon \zeta_3}, & \theta^* &= \theta e^{\epsilon \zeta_4} & f^* &= f e^{\epsilon \zeta_5} \end{aligned} \quad (19)$$

Now, $\epsilon \neq 0$ being a small parameter of the group, $(\zeta_1, \zeta_2, \zeta_3, \zeta_4, \zeta_5)$ are set of five real numbers and $(0,0,0,0,0)$ does not belong to the set. Then residuals of the Eq. (14) to Eq. (16) scaled down using Eq. (19) are

$$\varphi_1 = (1 + M^2) e^{\epsilon(2\zeta_2 - \zeta_3)} \frac{\partial^2 \psi^*}{\partial y^{*2}} - \lambda e^{\epsilon(\zeta_2 - \zeta_4)} \frac{\partial \theta^*}{\partial y^*} + Nr \lambda e^{\epsilon(\zeta_2 - \zeta_5)} \frac{\partial f^*}{\partial y^*} \quad (20)$$

$$\varphi_2 = e^{\epsilon(\zeta_1+\zeta_2-\zeta_3-\zeta_4)} \left(\frac{\partial \psi^*}{\partial y^*} \frac{\partial \theta^*}{\partial x^*} - \frac{\partial \psi^*}{\partial x^*} \frac{\partial \theta^*}{\partial y^*} \right) - e^{\epsilon(2\zeta_2-\zeta_4)} \frac{\partial^2 \theta^*}{\partial y^{*2}} - e^{\epsilon(3\zeta_2-\zeta_3-\zeta_4)} Pe_\gamma \left(\frac{\partial^2 \psi^*}{\partial y^{*2}} \frac{\partial \theta^*}{\partial y^*} + \frac{\partial^2 \theta^*}{\partial y^{*2}} \frac{\partial \psi^*}{\partial y^*} \right) - e^{\epsilon(2\zeta_2-\zeta_4-\zeta_5)} Nb \frac{\partial f^*}{\partial y^*} \frac{\partial \theta^*}{\partial y^*} - e^{\epsilon(2\zeta_2-2\zeta_4)} Nt \left(\frac{\partial \theta^*}{\partial y^*} \right)^2 - \frac{4}{3} R \frac{\partial}{\partial y^*} \left((C_T + e^{-\epsilon\zeta_4} \theta^*)^3 \frac{\partial \theta^*}{\partial y^*} \right) e^{\epsilon(2\zeta_2-\zeta_4)} \quad (21)$$

$$\varphi_3 = e^{\epsilon(\zeta_1+\zeta_2-\zeta_3-\zeta_5)} \left(\frac{\partial \psi^*}{\partial y^*} \frac{\partial f^*}{\partial x^*} - \frac{\partial \psi^*}{\partial x^*} \frac{\partial f^*}{\partial y^*} \right) - e^{\epsilon(2\zeta_2-\zeta_5)} \frac{1}{Le} \frac{\partial^2 f^*}{\partial y^{*2}} - e^{\epsilon(2\zeta_2-\zeta_4)} A \frac{\partial^2 \theta^*}{\partial y^{*2}} \quad (22)$$

Invariancy of Eq. (20) to Eq. (22) under Lie group transformations and further algebraic calculations is given by

$$\zeta_2 = \frac{\zeta_1}{2} = \zeta_3; \quad \zeta_4 = \zeta_5 = 0 \quad (23)$$

The scaling transformation Γ reduces as

$$\Gamma: x^* = xe^{\epsilon\zeta_1}, \quad y^* = ye^{\epsilon\frac{\zeta_1}{2}}$$

$$\psi^* = \psi e^{\epsilon\frac{\zeta_1}{2}}, \quad \theta^* = \theta, \quad f^* = f \quad (24)$$

The determinantal equations for the above set of residuals are

$$\frac{dx}{\zeta_1 x} = \frac{dy}{\epsilon\frac{\zeta_1}{2}y} = \frac{d\psi}{\epsilon\frac{\zeta_1}{2}\psi} = \frac{d\theta}{0} = \frac{df}{0} \quad (25)$$

The obtained similarity transformations are

$$\eta = yx^{-1/2}; \quad \psi = x^{\frac{1}{2}}H(\eta); \quad \theta = \theta(\eta); \quad f = f(\eta); \quad (26)$$

The ODE's on application of the above transformations on the Eq. (20) to Eq. (22)

$$(1 + M^2)H'' - \lambda\theta' + Nr\lambda f' = 0 \quad (27)$$

$$\theta'' + \frac{1}{2}H\theta' + Pe_\gamma(H''\theta' + H'\theta'') + Nb\theta'f' + Nt(\theta')^2 + \frac{4}{3}R((C_T + \theta)^3\theta')' = 0 \quad (28)$$

$$f'' + \frac{1}{2}LeHf' + \frac{Nt}{Nb}\theta'' = 0 \quad (29)$$

Where $A. Le = \frac{Nt}{Nb}$, being introduced in the last equation.

And the boundary conditions become

$$H(\eta) = 0; \quad \theta(\eta) = 1; \quad f(\eta) = 1 \quad \text{at} \quad \eta = 0 \quad (30)$$

$$H'(\eta) = 1; \quad \theta(\eta) = 0; \quad f(\eta) = 0 \quad \text{as} \quad \eta \rightarrow \infty \quad (31)$$

Local Nusselt number, local Sherwood number are prime focus of interest in various fields. It can be expressed as

$$Nu_x = \frac{xq_w}{k(\bar{T}_w - \bar{T}_\infty)} \quad , \quad Sh_x = \frac{xq_m}{k_f(\bar{\phi}_w - \bar{\phi}_\infty)} \quad (32)$$

where it can also be viewed as the following

$$\frac{Nu_x}{Pe^{1/2}} = - \left[1 + Pe_\gamma H'(0) + \frac{4}{3} R(C_{\bar{T}} + \theta(0))^3 \right] \theta'(0) \quad , \quad \frac{Sh_x}{Pe^{1/2}} = -f'(0) \quad (33)$$

3. Numerical Method

Obtained set of highly nonlinear ODE's (27) to (29), and boundary condition (30) to (31) is solved using the numerical calculations of shooting technique along with MATLAB bvp4c solver.

4. Results

Presentation of the similarity solutions of Eq. (27) to Eq. (29) and Eq. (30) and Eq. (31) using numerical technique called as Shooting method with bvp4c - scheme. When there is no impact of the magnetic parameter and radiation parameter, i.e., $M = 0; R = 0$, and the results have been compared to that of Meena [16] for varying values of Nt in Table 1.

Table 1

Comparison of the thermophoresis parameter values for the present study and of Meena [16] for $M = 0; R = 0$

Nt	Meena [16]	Present study
0.3	0.78574176	0.78574628
0.4	0.76711083	0.76711694

All the results have been explained and computed in the following ranges for the mentioned parameters

$$0.1 \leq Pe_\gamma \leq 2.0, 0.0 \leq Nr \leq 0.5, 0.1 \leq Nb \leq 0.5, 1.0 \leq Le \leq 1000, 0.1 \leq Nt \leq 0.5,$$

$$0.1 \leq \lambda \leq 3.0, 0.0 \leq R \leq 1.0, 0.0 \leq M \leq 2, 0.0 \leq C_{\bar{T}} \leq 0.3$$

Figure 2 to Figure 4 explains $H'(\eta)$, $\theta(\eta)$ and the profile of $f(\eta)$ for the variation of Nb for $\lambda = 1.0, Pe_\gamma = 0.5, R = 1.0, Nt = 0.1, C_{\bar{T}} = 0.1, Nr = 0.1, Le = 10, M = 1.0$. For the increment of Brownian motion parameter value, the molecular diffusion increases resulting in the decrement of the kinetic viscosity of the fluid and hence there is a rise in $H'(\eta)$ in Figure 4. The temperature increases and the rise in the fluid temperature aggregates in accelerating the velocity of the particles and subsiding the kinetic viscosity of the fluid as in Figure 3. The reduction in kinetic viscosity results in $f(\eta)$ reduction, being evident from Figure 2.

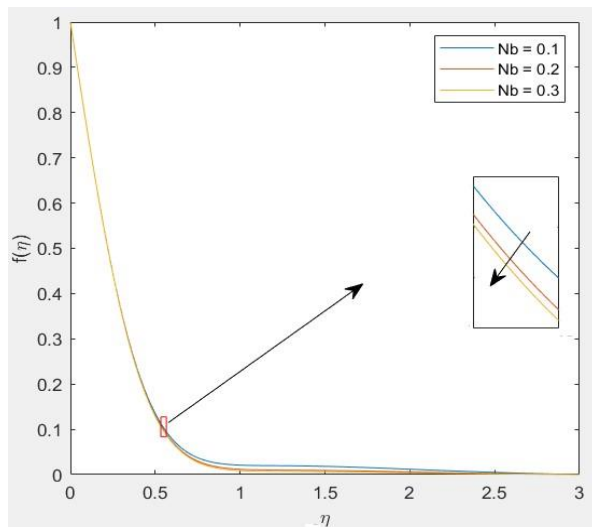


Fig. 2. $f(\eta)$ profile varying Nb

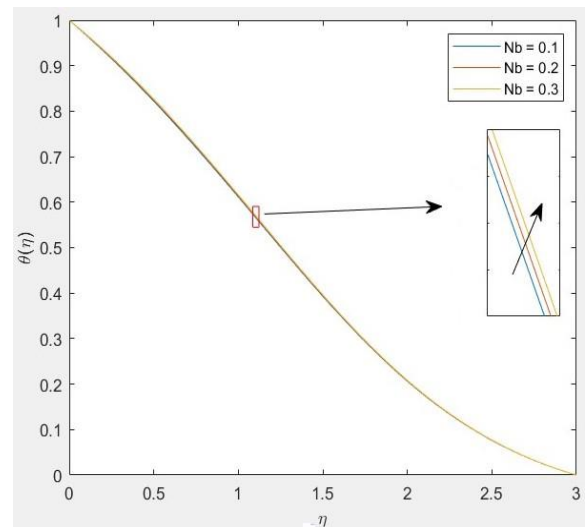


Fig. 3. $\theta(\eta)$ profile varying Nb

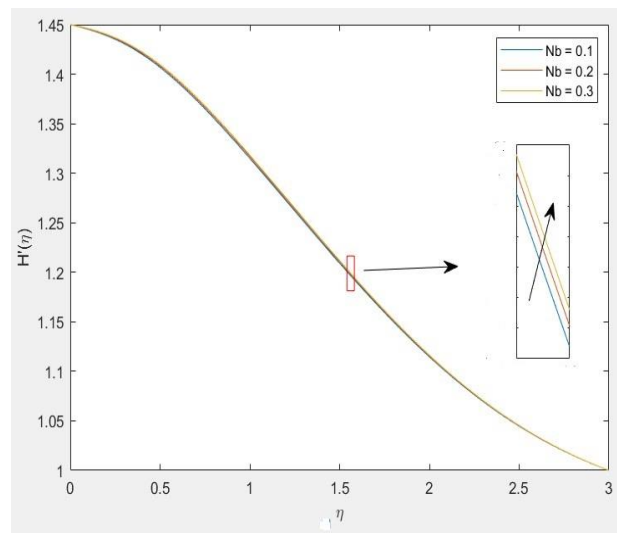


Fig. 4. $H'(\eta)$ profile varying Nb

Figure 5 to Figure 7 portraits the behaviour of $H'(\eta)$, $\theta(\eta)$ and $f(\eta)$ for the variation of Nt for $\lambda = 1.0, Pe_\gamma = 0.5, Nb = 0.3, Nr = 0.1, Le = 10, M = 1.0, C_{\bar{T}} = 0.1, R = 1.0$. Figure 7 shows roughly an increase in the $H'(\eta)$, profile by 0.27% while Figure 6 shows there is an increase of 1.7% in the values for the temperature profile $\theta(\eta)$. Due to this increase in the thermophoresis parameter value, there is an increase of about 28.5% in the $f(\eta)$ profile as shown in Figure 5. Physically, when a temperature difference is generated in the flow, the micro particles move faster in hotter regions and slower in colder regions. The collective effect of the differential dispersion of the particles apparently their migration from hotter to colder regions. The result of the migration is the accumulation of particles and higher particle concentrations in the colder regions of the particulate mixture. This is due to fact that Nt is directly proportional to the heat transfer coefficient associated with the fluid.

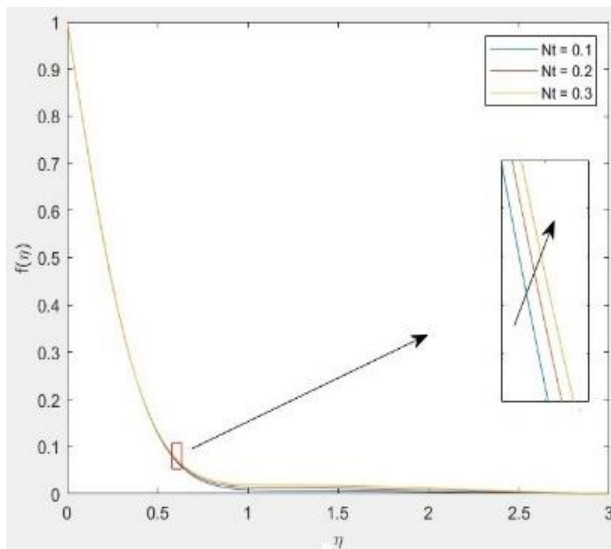


Fig. 5. $f(\eta)$ profile varying Nt

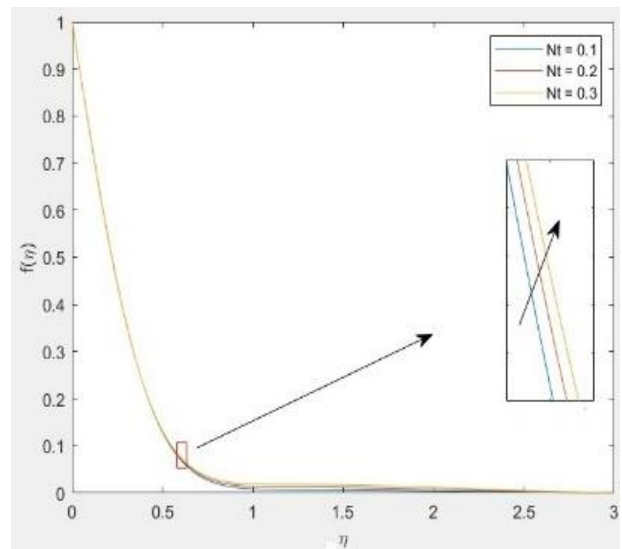


Fig. 6. $\theta(\eta)$ profile varying Nt

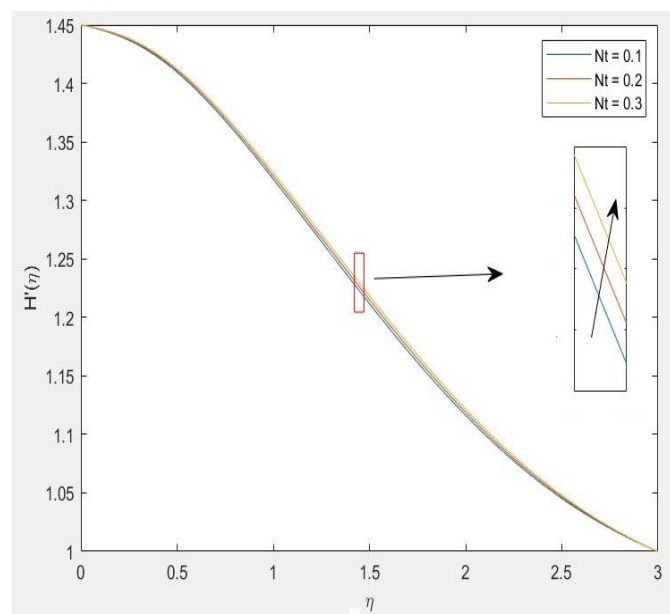


Fig. 7. $H'(\eta)$ profile varying Nt

Figure 8 to Figure 10 shows variation of $H'(\eta)$, $\theta(\eta)$ and $f(\eta)$ for the variation of R for $\lambda = 1.0$, $Pe_\gamma = 0.5$, $M = 1.0$, $Nb = 0.3$, $C_T = 0.1$, $Nr = 0.1$, $Le = 10$, $Nt = 0.1$. Figure 10 shows an increment in the $H'(\eta)$ profile by 2.22% while Figure 9 shows there is a rise of 13.5% in the values for the temperature profile $\theta(\eta)$. Physically an increment in radiation parameter causes the velocity of the fluid to rise. This is because as the radiation parameter is augmented, the heat absorption from the heated plate increases thus releasing more heat energy to the fluid while augmenting the temperature along with the buoyancy forces in the boundary layer. But as a reverse trend for this increase in the radiation parameter value, there is a decrease of around 8.2% in the $f(\eta)$ profile as shown in Figure 8.

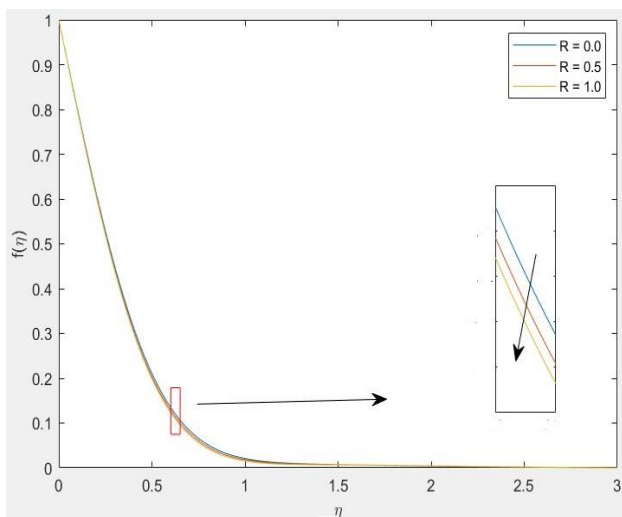


Fig. 8. $f(\eta)$ profile varying R

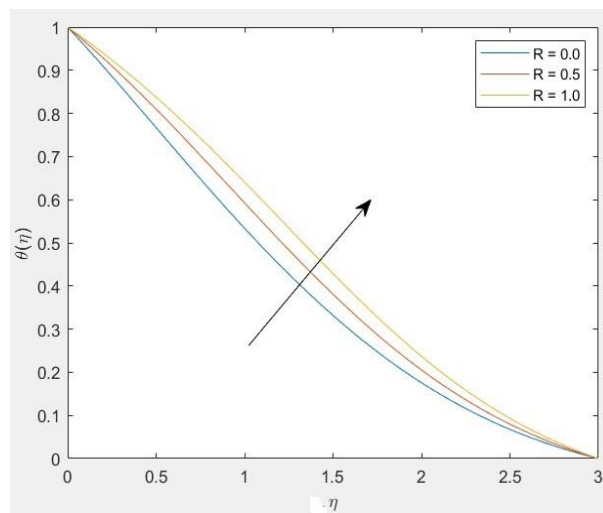


Fig. 9. $\theta(\eta)$ profile varying R

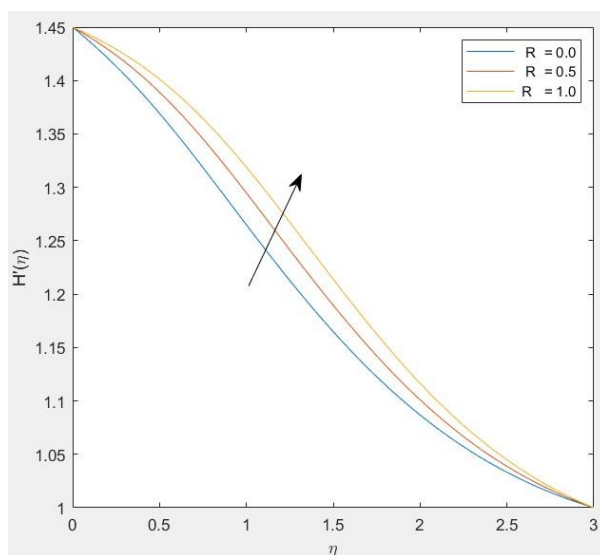


Fig. 10. $H'(\eta)$ profile varying R

Figure 11 to Figure 13 explains graphically the nature of $H'(\eta)$, $\theta(\eta)$ and $f(\eta)$ for the variation of M for $\lambda = 1.0$, $Pe_\gamma = 0.5$, $R = 1$, $Nb = 0.3$, $Nr = 0.1$, $Le = 10$, $C_{\bar{T}} = 0.1$, $Nt = 0.1$. Figure 11 shows a sharp increase in the $f(\eta)$ values by 44.9% when M changes from 0.1 to 0.2 but for the change of value from 0.2 – 0.3, the increase in the values was reduced to 25.16%. Figure 12 shows there is a rise of 2.4% in the values for $\theta(\eta)$ for the change in M value from 0.1 to 0.2 while an increase of 1.61% for the change from 0.2 to 0.3. For this change in the magnetic parameter value, there is a decrement in the $H'(\eta)$ profile as shown in Figure 13. Physically as M value shoots up, there is an amplification in the Lorentz force, and due to this hindrance, we can visualize that there will be a drop in the $f'(\eta)$ profile of the fluid flow which is clear from Figure 11. Numerically with the increase in the magnetic parameter value, the value of B increases, i.e., the strength of magnetic field increases that results in increase in Lorentz forces. With an escalation in the Lorentz force, the thickness of the thermal boundary layer decreases along with the Nusselt number (refer Table 2). Thus, centralization of the isothermal lines near the hot wall increases, thus showing a growth in the temperature profile as depicted in Figure 12.

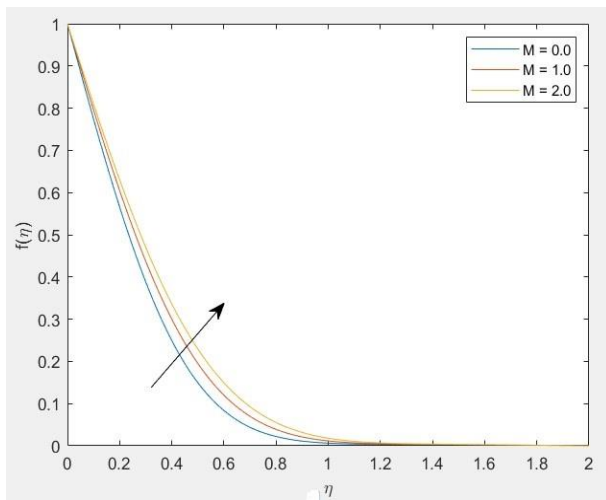


Fig. 11. $f(\eta)$ profile varying M

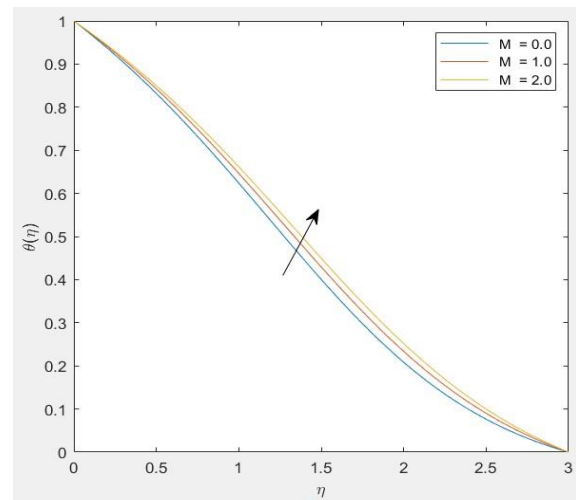


Fig. 12. $\theta(\eta)$ profile varying M

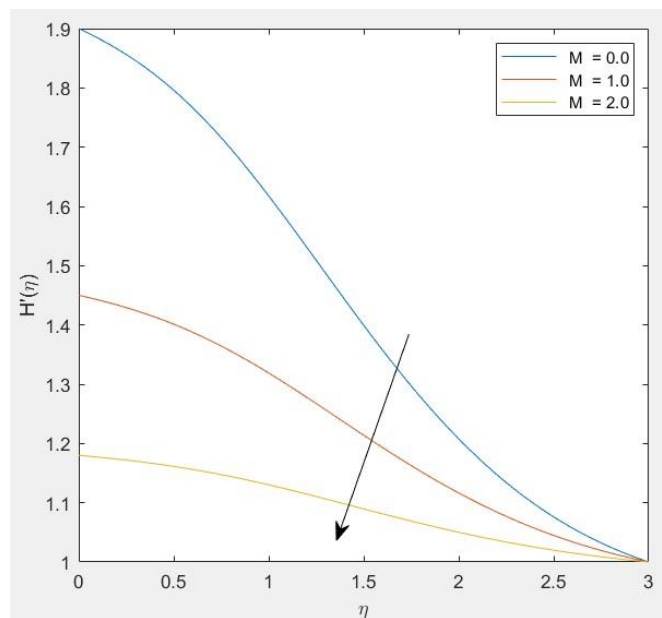


Fig. 13. $H'(\eta)$ profile varying M

Figure 14 to Figure 16 focusses on $H'(\eta)$, $\theta(\eta)$ and $f(\eta)$ for the variation of λ for $M = 1, Pe_\gamma = 0.5, R = 1, Nb = 0.3, Nr = 0.1, Le = 10, C_{\bar{T}} = 0.1, Nt = 0.1$. Figure 14 shows a decrement in the $f(\eta)$ profile by almost 28.9% by an increase in the mixed convection parameter. On a similar trend like $f(\eta)$, the temperature profile shows a downfall in its values by an average 2.3% by rise of λ because with the increase in the buoyancy effects, the convection cooling effect increases and hence the $\theta(\eta)$ value decreases as evident from Figure 15. To the contrast of the above observation from Figure 16, the $H'(\eta)$ profile shows a reverse trend where its value increases at the rate of 16.6% for an increment of $\lambda = 1.0$ to 2.0 by 16.6% and an increase of 13.6% for the further rise in the mixed convection parameter value. Physically, for the raise in the value of the parameter λ , the aiding flow velocity increases and the velocity for the opposing flow decreases. Hence as the λ value increases, the buoyancy effects increase and thus it accelerates the flow.

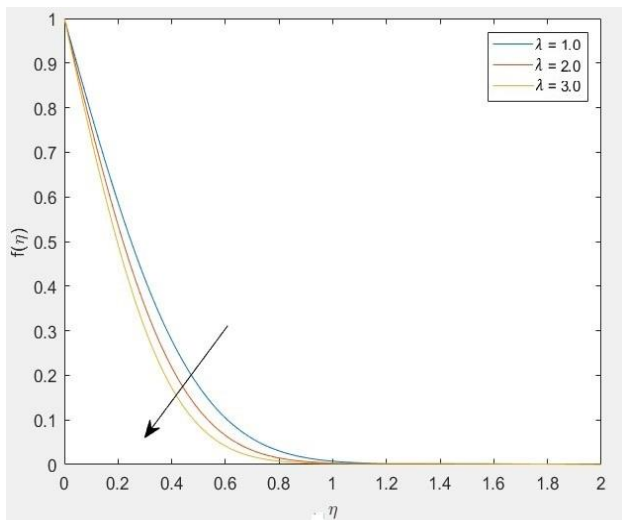


Fig. 14. $f(\eta)$ profile varying λ

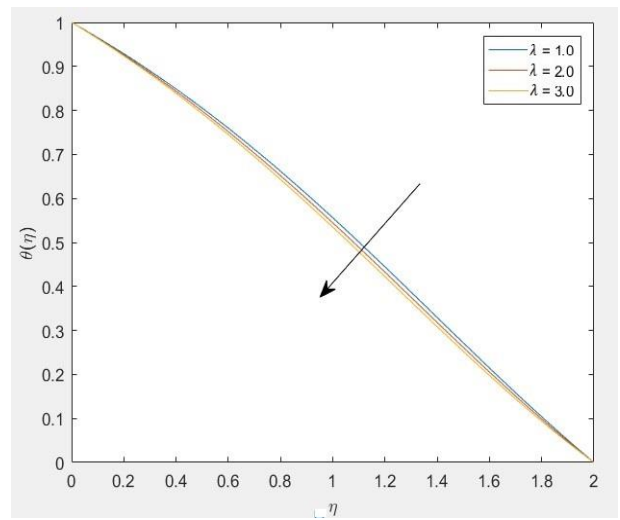


Fig. 15. $\theta(\eta)$ profile varying λ

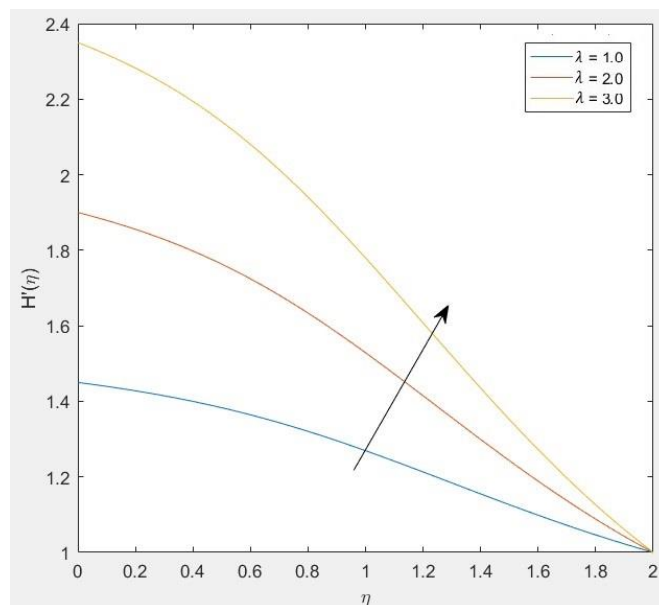


Fig. 16. $H'(\eta)$ profile varying λ

Figure 17 to Figure 19 describes $H'(\eta)$, $\theta(\eta)$ and $f(\eta)$ profile changes for the variation of Le for $M = 1, Pe_\gamma = 0.5, C_{\bar{T}} = 0.1, Nb = 0.3, Nr = 0.1, Le = 10, R = 1, Nt = 0.1$. Figure 17 shows a very sharp decrease in the $f(\eta)$ profile by almost 70% by an increase in the Lewis number parameter. It is clearly observed that the nanoparticles volume fraction as well as its boundary-layer thickness increase considerably as Le increases. Similarly, like $f(\eta)$, the temperature profile shows a downfall in its values by an average 3.17% as λ value grows as evident from Figure 18. But from Figure 19, the $H'(\eta)$ profile shows a reverse trend where its value increases for the increase in the Lewis number parameter value.

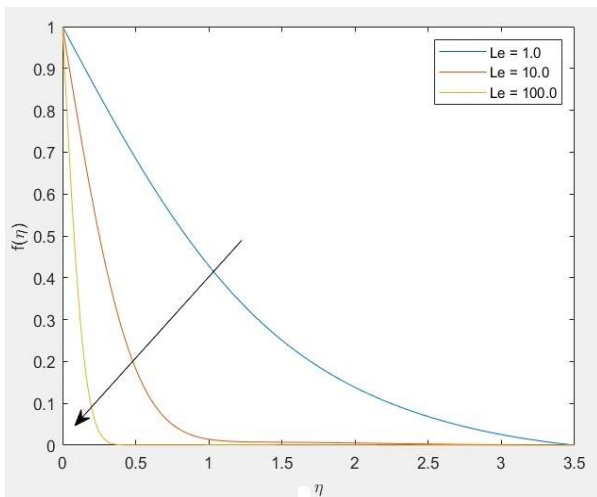


Fig. 17. $f(\eta)$ profile varying Le

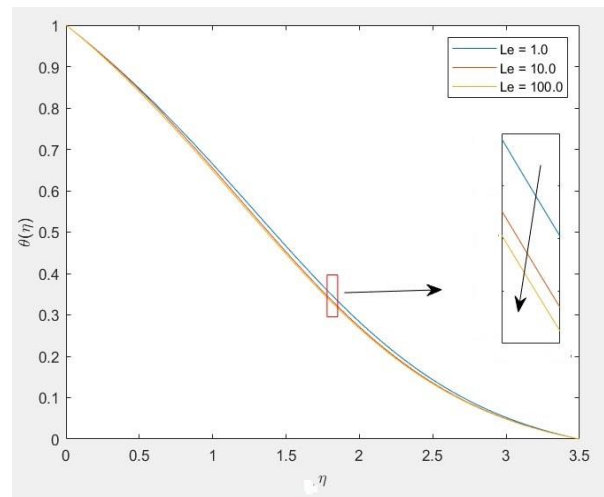


Fig. 18. $\theta(\eta)$ profile varying Le

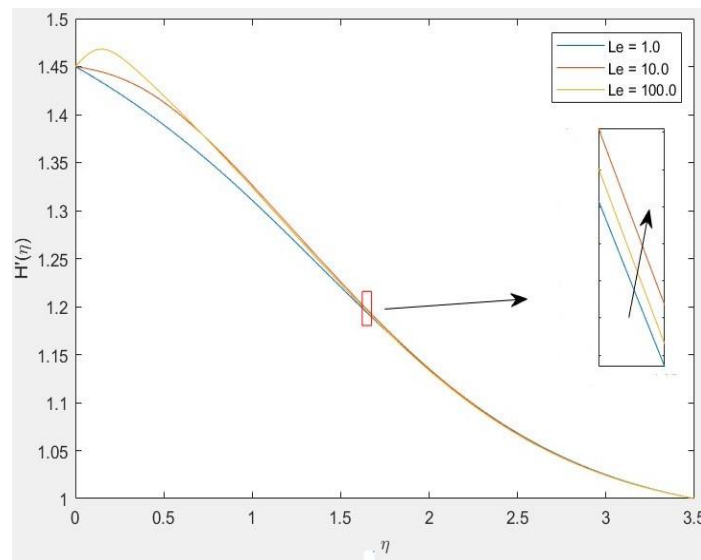


Fig. 19. $H'(\eta)$ profile varying Le

From the Table 2, we will observe the behavior of the local Sherwood and Nusselt number due to the variation in the impact parameters with all other parameters having a fixed value.

Table 2

Nusselt number and Sherwood number for varying values of Nt, R, M, Nb when $Le = 10.0, Ct = 0.1, Pe_\gamma = 0.5, \lambda = 1.0, Nr = 0.1$

M	Nb	Nt	R	$-\theta'(0)$	$-f'(0)$
0.0	0.3	0.1	1.0	0.347172	2.468260
1.0	0.3	0.1	1.0	0.334424	2.167720
2.0	0.3	0.1	1.0	0.326119	1.967790
1.0	0.1	0.1	1.0	0.353270	2.221540
1.0	0.2	0.1	1.0	0.343709	2.180970
1.0	0.3	0.1	1.0	0.334424	2.167720
1.0	0.3	0.2	1.0	0.328403	2.204800
1.0	0.3	0.3	1.0	0.322538	2.244540
1.0	0.3	0.4	1.0	0.316824	2.286940
1.0	0.3	0.1	0.0	0.507121	2.120670
1.0	0.3	0.1	0.5	0.393830	2.151970
1.0	0.3	0.1	1.0	0.334424	2.167720

5. Conclusions

Using the tool of Lie group scaling we have obtained the similarity solutions for the highly nonlinear set of PDE's along with its boundary conditions converting them to a set of ODE's.

- i. For increasing M increases, Nu_x and Sh_x increases along with the increment of $\theta(\eta)$ and $f(\eta)$ profiles. But with M increasing, the velocity profile $H'(\eta)$ falls.
- ii. With the increment Nt value there is a rise in Sh_x but Nu_x decreases. On the other hand, with the increasing Nt value each of the $H'(\eta)$, $\theta(\eta)$ and $f(\eta)$ shows an increasing profile.
- iii. For the increasing value of Nb , as a similar trend to M , both Nu_x and Sh_x decreases. The nanoparticle volume fraction $f(\eta)$ decreases while with a reverse nature the $H'(\eta)$ and $\theta(\eta)$ graphs experience a rise in value.
- iv. There is an increase in Sh_x value and Nu_x value decreases with increasing R parameter. Like the behaviour of Nb , the velocity profile $H'(\eta)$ and $\theta(\eta)$ increases while $f(\eta)$ decreases.

The present study has been conducted on a vertical wedge with for mixed convection with varying effects like thermal dispersion, radiation, magnetisation and Brownian motion. As a future scope, these concepts can be further improvised and can be applied on various other geometries like vertical plates, cones etc. along with the use of different types of fluids with the influence of free or forced convection.

Acknowledgement

This research was not funded by any grant.

References

- [1] Gorla, R. S. R., and M. Kumari. "Mixed convection in non-Newtonian fluids along a vertical plate in a porous medium." *Acta Mechanica* 118, no. 1 (1996): 55-64. <https://doi.org/10.1007/BF01410507>
- [2] Reddy, P. Sudarsana, and A. J. Chamkha. "Heat and mass transfer characteristics of nanofluid over horizontal circular cylinder." *Ain Shams Engineering Journal* 9, no. 4 (2018): 707-716. <https://doi.org/10.1016/j.asej.2016.03.015>
- [3] Selimefendigil, Fatih, and Hakan F. Öztop. "Numerical study of MHD mixed convection in a nanofluid filled lid driven square enclosure with a rotating cylinder." *International Journal of Heat and Mass Transfer* 78 (2014): 741-754. <https://doi.org/10.1016/j.ijheatmasstransfer.2014.07.031>
- [4] Khan, Waqar A., and I. Pop. "Boundary layer flow past a wedge moving in a nanofluid." *Mathematical Problems in Engineering* 2013 (2013). <https://doi.org/10.1155/2013/637285>
- [5] Turkyilmazoglu, M. "Exact analytical solutions for heat and mass transfer of MHD slip flow in nanofluids." *Chemical Engineering Science* 84 (2012): 182-187. <https://doi.org/10.1016/j.ces.2012.08.029>
- [6] Khan, Md Shakhaoath, Ifsana Karim, Md Sirajul Islam, and Mohammad Wahiduzzaman. "MHD boundary layer radiative, heat generating and chemical reacting flow past a wedge moving in a nanofluid." *Nano Convergence* 1, no. 1 (2014): 1-13. <https://doi.org/10.1186/s40580-014-0020-8>
- [7] Nield, Donald A., and Adrian Bejan. *Convection in porous media*. Vol. 3. New York: Springer, 2006.
- [8] Murthy, P. V. S. N., and P. Singh. "Thermal dispersion effects on non-Darcy natural convection with lateral mass flux." *Heat and Mass Transfer* 33, no. 1 (1997): 1-5. <https://doi.org/10.1007/s002310050155>
- [9] Pranitha, Janapatla, G. Venkata Suman, and Darbhasayanam Srinivasacharya. "Numerical Study on Mixed Convection in a Power-Law Fluid Saturated Porous Medium with Variable Properties and Thermophoresis Effects via Lie Scaling Group Transformations." *Computational Thermal Sciences: An International Journal* 10, no. 6 (2018). <https://doi.org/10.1615/ComputThermalScien.2018016882>
- [10] Meena, Om Prakash, and J. Pranitha. "Power-law nanofluid on mixed convection with influence of double dispersion saturated non-Darcy porous media." In *AIP Conference Proceedings*, vol. 2246, no. 1, p. 020019. AIP Publishing LLC, 2020. <https://doi.org/10.1063/5.0014503>

- [11] Buongiorno, Jacopo. "Convective transport in nanofluids." *ASME Journal of Heat and Mass Transfer* 128, no. 3 (2006): 240-250. <https://doi.org/10.1115/1.2150834>
- [12] Khan, Umar, Naveed Ahmed, Bandar Bin-Mohsen, and Syed Tauseef Mohyud-Din. "Nonlinear radiation effects on flow of nanofluid over a porous wedge in the presence of magnetic field." *International Journal of Numerical Methods for Heat & Fluid Flow* (2017). <https://doi.org/10.1108/HFF-10-2015-0433>
- [13] Brewster, M. Quinn. *Thermal radiative transfer and properties*. John Wiley & Sons, 1992.
- [14] Pranitha, J., G. Venkata Suman, and D. Srinivasacharya. "Scaling Group Transformation for Mixed Convection in a Power-Law Fluid Saturated Porous Medium with Effects of Soret, Radiation and Variable Properties." *Frontiers in Heat and Mass Transfer* 9, no. 39 (2017): 1-8. <https://doi.org/10.5098/hmt.9.39>
- [15] Chamkha, Ali J., S. Abbasbandy, A. M. Rashad, and K. Vajravelu. "Radiation effects on mixed convection over a wedge embedded in a porous medium filled with a nanofluid." *Transport in Porous Media* 91, no. 1 (2012): 261-279. <https://doi.org/10.1007/s11242-011-9843-5>
- [16] Meena, Om Prakash. "Mixed convection nanofluid flow over a vertical wedge saturated in porous media with the influence of thermal dispersion using Lie group scaling." *Computational Thermal Sciences: An International Journal* 12, no. 3 (2020): 191-205. <https://doi.org/10.1615/ComputThermalScien.2020032330>
- [17] Ganga, B., S. Mohamed Yusuff Ansari, N. Vishnu Ganesh, and A. K. Abdul Hakeem. "Hydromagnetic flow and radiative heat transfer of nanofluid past a vertical plate." *Journal of Taibah University for Science* 11, no. 6 (2017): 1200-1213. <https://doi.org/10.1016/j.jtusci.2015.12.005>
- [18] Cavallini, Alberto, Davide Del Col, Luca Doretti, Giovanni Antonio Longo, and Luisa Rossetto. "A new computational procedure for heat transfer and pressure drop during refrigerant condensation inside enhanced tubes." *Journal of Enhanced Heat Transfer* 6, no. 6 (1999). <https://doi.org/10.1615/JEnhHeatTransf.v6.i6.50>
- [19] Divya, B. B., G. Manjunatha, C. Rajashekhar, Hanumesh Vaidya, and K. V. Prasad. "Analysis of temperature dependent properties of a peristaltic MHD flow in a non-uniform channel: A Casson fluid model." *Ain Shams Engineering Journal* 12, no. 2 (2021): 2181-2191. <https://doi.org/10.1016/j.asej.2020.11.010>
- [20] Prasad, K. V., Hanumesh Vaidya, C. Rajashekhar, Sami Ullah Khan, G. Manjunatha, and J. U. Viharika. "Slip flow of MHD Casson fluid in an inclined channel with variable transport properties." *Communications in Theoretical Physics* 72, no. 9 (2020): 095004. <https://doi.org/10.1088/1572-9494/aba246>
- [21] Vaidya, Hanumesh, C. Rajashekhar, K. V. Prasad, Sami Ullah Khan, Arshad Riaz, and J. U. Viharika. "MHD peristaltic flow of nanofluid in a vertical channel with multiple slip features: an application to chyme movement." *Biomechanics and Modeling in Mechanobiology* 20, no. 3 (2021): 1047-1067. <https://doi.org/10.1007/s10237-021-01430-y>
- [22] Vaidya, H., C. Rajashekhar, K. V. Prasad, S. U. Khan, F. Mebarek-Oudina, A. Patil, and P. Nagathan. "Channel flow of MHD bingham fluid due to peristalsis with multiple chemical reactions: an application to blood flow through narrow arteries." *SN Applied Sciences* 3, no. 2 (2021): 1-12. <https://doi.org/10.1007/s42452-021-04143-0>
- [23] Yen, Wah Tey, Yutaka Asako, Nor Azwadi Che Sidik, and Goh Rui Zher. "Governing equations in computational fluid dynamics: Derivations and a recent review." *Progress in Energy and Environment* 1 (2017): 1-19.
- [24] Khan, Ansab Azam, Khairy Zaimi, Suliadi Firdaus Sufahani, and Mohammad Ferdows. "MHD flow and heat transfer of double stratified micropolar fluid over a vertical permeable shrinking/stretching sheet with chemical reaction and heat source." *Journal of Advanced Research in Applied Sciences and Engineering Technology* 21, no. 1 (2020): 1-14. <https://doi.org/10.37934/araset.21.1.114>
- [25] Asghar, Adnan, and Yuan Ying Teh. "Three dimensional MHD hybrid nanofluid Flow with rotating stretching/shrinking sheet and Joule heating." *CFD Letters* 13, no. 8 (2021): 1-19. <https://doi.org/10.37934/cfdl.13.8.119>
- [26] Bakar, Fairul Naim Abu, and Siti Khuzaimah Soid. "MHD Stagnation-Point Flow and Heat Transfer Over an Exponentially Stretching/Shrinking Vertical Sheet in a Micropolar Fluid with a Buoyancy Effect." *Journal of Advanced Research in Numerical Heat Transfer* 8, no. 1 (2022): 50-55.
- [27] Thirupathi, Gurralla, Kamatam Govardhan, and Ganji Narender. "Radiative Magnetohydrodynamics Casson Nanofluid Flow and Heat and Mass Transfer past on Nonlinear Stretching Surface." *Journal of Advanced Research in Numerical Heat Transfer* 6, no. 1 (2021): 1-21. <https://doi.org/10.3762/bxiv.2021.65.v1>
- [28] Akaje, T. W., and B. I. Olajuwon. "Impacts of Nonlinear thermal radiation on a stagnation point of an aligned MHD Casson nanofluid flow with Thompson and Troian slip boundary condition." *Journal of Advanced Research in Experimental Fluid Mechanics and Heat Transfer* 6, no. 1 (2021): 1-15.